

Aberystwyth University

The evolutionary genomics of anthroponosis in Cryptosporidium

Nader, Johanna ; Mathers, Thomas; Ward, Ben; Pachebat, Justin Alexander; Swain, Martin; Robinson, Guy; Chalmers, Rachel M.; Hunter, Paul R.; van Oosterhout, Cock; Tyler, Kevin

Published in:
Nature Microbiology

DOI:
[10.1038/s41564-019-0377-x](https://doi.org/10.1038/s41564-019-0377-x)

Publication date:
2019

Citation for published version (APA):

Nader, J., Mathers, T., Ward, B., Pachebat, J. A., Swain, M., Robinson, G., Chalmers, R. M., Hunter, P. R., van Oosterhout, C., & Tyler, K. (2019). The evolutionary genomics of anthroponosis in *Cryptosporidium*. *Nature Microbiology*, 4(N/A), 826-836. <https://doi.org/10.1038/s41564-019-0377-x>

General rights

Copyright and moral rights for the publications made accessible in the Aberystwyth Research Portal (the Institutional Repository) are retained by the authors and/or other copyright owners and it is a condition of accessing publications that users recognise and abide by the legal requirements associated with these rights.

- Users may download and print one copy of any publication from the Aberystwyth Research Portal for the purpose of private study or research.
- You may not further distribute the material or use it for any profit-making activity or commercial gain
- You may freely distribute the URL identifying the publication in the Aberystwyth Research Portal

Take down policy

If you believe that this document breaches copyright please contact us providing details, and we will remove access to the work immediately and investigate your claim.

tel: +44 1970 62 2400
email: is@aber.ac.uk

1 Title: Evolutionary genomics of anthroponosis in *Cryptosporidium*

2
3 Authors and Affiliations

4 Johanna L. Nader^{1,2}, Thomas C. Mathers³, Ben J. Ward^{3,4}, Justin A. Pachebat⁵, Martin T.
5 Swain⁵, Guy Robinson^{6,7}, Rachel M. Chalmers^{6,7}, Paul R. Hunter¹, Cock van Oosterhout^{4*},
6 Kevin M. Tyler^{1*}

7
8 ¹Biomedical Research Centre, Norwich Medical School, University of East Anglia, Norwich, United Kingdom

9 ²Department of Genetics and Bioinformatics, Division of Health Data and Digitalisation, Norwegian Institute of
10 Public Health, Oslo, Norway

11 ³Earlham Institute, Norwich Research Park, Norwich, United Kingdom

12 ⁴School of Environmental Sciences, Norwich Research Park, University of East Anglia, United Kingdom

13 ⁵Institute of Biological, Environmental & Rural Sciences, Aberystwyth University, Aberystwyth, United
14 Kingdom

15 ⁶*Cryptosporidium* Reference Unit, Public Health Wales Microbiology, Singleton Hospital, Swansea, United
16 Kingdom

17 ⁷Swansea University Medical School, Singleton Park, Swansea, United Kingdom

18
19 *Contributed equally to the work

20
21
22
23 Corresponding authors:

24 Email: johanna.nader@fhi.no

25 Telephone: +47 41221727

26 Address: Norwegian Institute of Public Health, Postbox 4404, Nydalen 0403, Oslo, Norway

27
28 Email: c.van-oosterhout@uea.ac.uk

29 Telephone: +44 1603 592921

30 Address: School of Environmental Sciences, University of East Anglia, Norwich Research Park, Norwich NR4
31 7TJ, UK

32
33
34
35
36
37
38
39
40
41
42
43
44
45
46
47
48
49
50
51
52

53

54 **Abstract**

55 Human cryptosporidiosis is the leading protozoan cause of diarrhoeal mortality worldwide,
56 and a preponderance of infections is caused by *Cryptosporidium hominis* and *C. parvum*.
57 Both species consist of several subtypes with distinct geographic distributions and host
58 preferences (i.e. generalist zoonotic and specialist anthroponotic subtypes). The evolutionary
59 processes driving the adaptation to human host, and the population structure remain
60 unknown. In this study, we analyse 21 whole genome sequences to elucidate the evolution of
61 anthroponosis. We show that *C. parvum* splits into two subclades, and that the specialist
62 anthroponotic subtype IIc-a shares a subset of loci with *C. hominis* that are undergoing rapid
63 convergent evolution driven by positive selection. Subtype IIc-a also has an elevated level of
64 insertion-deletion (indel) mutations in the peri-telomeric genes, which is characteristic also
65 for other specialist subtypes. Genetic exchange between subtypes plays a prominent role
66 throughout the evolution of *Cryptosporidium*. Interestingly, recombinant regions are enriched
67 for positively selected genes and potential virulence factors, which indicates adaptive
68 introgression. Analysis of 467 gp60 sequences collected across the world shows that the
69 population genetic structure differs markedly between the main zoonotic subtype (isolation-
70 by-distance) and the anthroponotic subtype (admixed population structure). Finally, we show
71 that introgression between the four anthroponotic *Cryptosporidium* subtypes and species
72 included in this study has occurred recently, probably within the past millennium.

73

74 **Introduction**

75 Diarrhoeal pathogens cause more mortality than malaria, measles, and AIDS combined¹ and
76 globally, for children under five, *Cryptosporidium* is the leading, vaccine non-preventable
77 cause of diarrhoeal morbidity and mortality². The zoonotic *Cryptosporidium parvum* and the
78 anthroponotic *Cryptosporidium hominis* account for a vast majority of such cases. *C. hominis*
79 and *C. parvum* have consistently been reported as exhibiting a high average global consensus
80 of ~95-97% nucleotide identities^{3,4}; yet, the genetic basis for the difference in host range has
81 remained unexplained, and our understanding of host adaptation is confounded by the
82 existence of anthroponotic *C. parvum* isolates (Supplementary Fig. S1). The relatively high
83 level of genomic conservation between these species could be explained by similarity in
84 selection pressures experienced by these parasites that is irrespective of their hosts. For
85 example, *Plasmodium berghei* requires two-thirds of genes for optimal growth during a
86 single stage of its complex life cycle⁵. Alternatively, hybridization amongst isolates of
87 *Cryptosporidium* species could lead to genetic introgression that homogenizes sequence
88 variation. For example, some “generalist” plant pathogens such as the oomycete *Albugo*
89 *candida* have a huge host range consisting of hundreds of plant species that are parasitized by
90 host-specific subtypes⁶. This pathogen suppresses the immune response of the host plant,
91 enabling hybridization between different subtypes leading to genetic introgression that is
92 thought to fuel the coevolutionary arms race³⁸. Similarly, in the mosaic-like *Toxoplasma*
93 *gondii* genomes there are conserved chromosomal haploblocks which are shared across
94 otherwise diverged clades⁷.

95

96 The ~9.14Mbp *Cryptosporidium* genome comprises 8 chromosomes ranging in size from
97 0.88 to 1.34Mbp, and has a highly compact coding sequence composition (73.2-77.6%)⁸.
98 Genomic comparisons between the original *C. parvum* Iowa⁹ and *C. hominis* TU502¹⁰
99 reference genomes currently provide an overview of chromosome-wide hotspots for single
100 nucleotide polymorphisms (SNPs), selective pressures, and species-specific genes and
101 duplication events^{4,11}. These studies revealed peri-telomeric clustering of hyper-
102 polymorphism and identified several putative virulence factors. Attempts to correlate

103 genomic changes with phenotypic expression identified only a few shared SNPs between the
104 anthroponotic *C. parvum* and *C. hominis*¹². Whole genome comparisons found genome-wide
105 incongruence and significant sequence insertion and deletion (indels) events between *C.*
106 *hominis* and *C. parvum*¹³, and recombination at the hypervariable gp60 subtyping locus¹⁴.
107 Expanding cross-comparisons to include multiple whole genome sequences (WGS) across a
108 range of anthroponotic and zoonotic *C. parvum* and *C. hominis* strains will help to explore
109 these phenotype-associated features, and understand the evolution of human-infective strains.

110
111 Here, we have conducted a phylogenetic comparison of 21 WGS, including 11 previously
112 unpublished *Cryptosporidium* genome sequences (Table S1). In addition, we characterise the
113 global distribution of *Cryptosporidium* species and subtypes, summarising the data of 743
114 peer-reviewed publications of cases in a total of 126 countries that used the gp60 locus for
115 species identification and subtyping. We describe the evolutionary genomic changes of this
116 pathogen during its association with its human host and host-range specialisation, and we
117 estimate divergence times for the primary anthroponotic lineages. Our analyses provide a
118 revised evolutionary scenario supporting the more recent emergence of a previously cryptic,
119 phylogenetically-distinct anthroponotic *Cryptosporidium parvum anthroponosum* sub-
120 species.

121 122 **Results**

123
124 A phylogenetic analysis of 61 neutrally-evolving coding loci across 21 *Cryptosporidium*
125 isolates reveals the evolutionary history of human-infective taxa and identifies two discrete
126 *C. parvum* lineages with distinct host associations, namely *C. p. parvum* (zoonotic) and *C. p.*
127 *anthroponosum* (anthroponotic) (Fig. 1a; Fig. S1)¹³. Primary human-infective isolates¹⁵ *C.*
128 *hominis* and *C. parvum* form a distinct superclade with zoonotic *C. cuniculus*, a recently-
129 identified cause of human outbreaks^{16,17}. This superclade is genetically distinct from other
130 zoonotic human-infectious *Cryptosporidium* species (*C. meleagridis*¹⁸, *C. viatorum*¹⁹, *C.*
131 *ubiquitum*²⁰, *C. baileyi*²¹ and *C. muris*²²; Fig. 1a; Fig. S2; absolute divergence (d_{xy}) = 0.083 –
132 0.478). Within the superclade, limited genetic divergence between *C. hominis* and *C. parvum*
133 (d_{xy} = 0.031) illustrates the recent origins of these taxa. Finally, the concatenated phylogeny
134 provides a preliminary genotypic association between phenotypically-diverse *C. parvum*
135 strains. Based on the host ranges of a total of 1331 isolates, *C. p. anthroponosum* UKP15
136 (subtype IIc-a) is almost exclusively found in humans (92.2%), whereas *C. p. parvum* UKP6
137 and UKP8 (subtypes IIa and IIc, respectively) are more often found in ruminants than in
138 humans (Fig. 1S). These zoonotic subtypes (UKP6 and UKP8) split off into a unique sister
139 group (*C. p. parvum*) within the *C. parvum* clade, distinct from the anthroponotic subtype (*C.*
140 *p. anthroponosum*). This switch in host association is associated with surprisingly low levels
141 of genetic divergence (d_{xy} = 0.002), suggesting it happened recently.

142
143 Next, we undertook a meta-analysis to establish the distribution and population genetics of
144 these *Cryptosporidium* species and subtypes based on gp60 genotyping, summarising the data
145 of 743 peer-reviewed publications of cases in a total of 126 countries worldwide published
146 between 2000 and 2017. The anthroponotic species *C. hominis* and *C. p. anthroponosum* are
147 relatively more prevalent in resource poor countries (Fig. 1b,c). In contrast, the zoonotic *C. p.*
148 *parvum* dominates in North America, Europe, parts of the Middle East and Australia. Even
149 though *C. p. anthroponosum* is less prevalent in Europe (17%; 22 out of 128 cases), the mean
150 nucleotide diversity at gp60 is significantly higher than that of *C. p. parvum* (π = 0.02954 vs.
151 0.00327, respectively) (Mann-Whitney test: $W = 430412$; $p < 10^{-5}$) (Fig. 1d). The population
152 genetic structure differs significantly between *C. p. anthroponosum* and *C. p. parvum* (GLM:

153 $F_{1,79} = 47.34$, $p < 0.0001$), with *C. p. parvum* showing a strong isolation-by-distance signal,
154 whereas there is no geographic population genetic structure for *C. p. anthroponosum* (Fig. 1e;
155 Tables S2, S3). In Europe, *C. p. parvum* forms a geographically-structured population which
156 shows significant isolation-by-distance (Fig. 1f,g). This suggests that gene flow within
157 Europe shapes the genetic differentiation (F_{st}) of *C. p. parvum*, and that this pathogen is
158 transmitted between European countries. In contrast, the high nucleotide diversity and lack of
159 geographic structuring implies that *C. p. anthroponosum* may be introduced in Europe from
160 genetically diverged source populations. The population genetic structure of both species is
161 also different when analysed across a global-scale, with network analysis revealing
162 significant sub-structuring of global populations of *C. p. parvum*, but not of *C. p.*
163 *anthroponosum* (Fig. 1g,h).

164
165 Nucleotide divergence between *C. p. parvum* and *C. p. anthroponosum* is driven partly by
166 positive selection, as evidenced by the relatively elevated ratio of Ka/Ks (> 1.0) for 44 loci
167 (Fig. 2a; Table S4). The Ka/Ks ratio between the *C. p. parvum* subspecies is comparable to the
168 Ka/Ks ratio of *C. p. parvum* and *C. hominis* comparison, and significantly higher than the
169 Ka/Ks ratio of comparisons between other *C. p. parvum* subtypes (Fig. 2b). The signature of
170 adaptive evolution is most apparent in the peri-telomeric genes (Fig. S4). Furthermore,
171 frameshift-causing indels also underpin protein divergence in 130 (55.6%) and 24 (53.3%)
172 variable *C. hominis* and *C. p. anthroponosum* amino acid coding sequences, respectively
173 (Table S5, S6). When accounting for the size of the different chromosomal regions, indels are
174 significantly more common in the peri-telomeric and subtelomeric regions than elsewhere in
175 the genome (Chi-sq. test: $X^2 = 257.71$, $df = 2$, $p = 1.09 \times 10^{-56}$) (Fig. 2c). Genes encoding for
176 extracellular proteins show a significantly stronger signal of positive selection than genes
177 with a cytoplasmic protein localization (Mann-Whitney test: $W = 842985$, $p = 0.0182$) (Fig.
178 2d; S5), consistent with adaptations/specialisation to the human host.

179
180 Besides nucleotide substitutions and indels, genetic introgression also appears to play a
181 prominent role in the adaptive evolution of *Cryptosporidium*. To investigate genome-wide
182 patterns of divergence between *Cryptosporidium* lineages we aligned reads from 16 isolates
183 to the *C. parvum* Iowa reference genome⁹. Principle component analysis based on a set high
184 quality SNPs supports the sub-species assignments of zoonotic *C. p. parvum* and
185 anthroponotic *C. p. anthroponosum* (Fig. 3a). Surprisingly, one sample (UKP16), identified
186 as *C. p. parvum* based on phylogenetic analysis of 61 single copy conserved genes (Fig. 1a),
187 appears to be highly differentiated based on genome wide SNPs (Fig. 3a). To further
188 investigate the evolutionary history of this sample we generated phylogenetic trees in 50 SNP
189 windows across the genome. The consensus topology of these genomic windows is shown as
190 a “cloudogram” (Fig. 3b), which matches the concatenated analysis of conserved protein
191 coding genes (Fig. 1a), with UKP16 most closely related to *C. p. parvum* isolates. However,
192 many alternative topologies are also observed, indicating potential recombination between
193 lineages (Fig. 3b). We used topology weighting²³ to visualise the distribution of topologies
194 across the genome, focusing on evolutionary relationships between UKP16, *C. p. parvum*
195 isolates and *C. p. anthroponosum* isolates (Fig. 3c). This analysis revealed a large region in
196 chromosome 8 (~500 - 650Kb) where UKP16 has a sister relationship to *C. p. parvum*
197 isolates and *C. p. anthroponosum* isolates (topo1; Fig. 3c and d). Intriguingly, this appears to
198 be due introgression into the UKP16 genome from a highly divergent, and as yet unsampled,
199 lineage. We draw this conclusion because the absolute divergence (d_{xy}) between UKP16 and
200 both *C. p. anthroponosum* and *C. p. parvum* is elevated in this region, whereas divergence
201 between *C. p. anthroponosum* and *C. p. parvum* is similar to the rest of the chromosome (Fig.
202 3e).

203

204 Next, we conducted a detailed analysis of genetic introgression, studying two *C. parvum*
205 *parvum* isolates (UKP6 and UKP16), one *C. parvum anthroponosum* isolate (UKP15), and
206 one *C. hominis* isolate (UKH1). A total of 104 unique recombination events are detected
207 across these four whole genome sequences (Fig 4a; Table S7). Many recombination events
208 involve an unknown parental sequence (i.e. donor), which is consistent with our findings for
209 the UKP16 sample, where we identified an introgressed genomic segment from a diverged
210 lineage (see above). These results highlight that genetic exchange is widespread across
211 *Cryptosporidium* species. The distribution of recombination events varies markedly across
212 chromosomes, with a disproportionately higher number of individual events detected in
213 chromosome 6 (25.9% of total events), and a disproportionately lower number of events in
214 chromosomes 3, 5, and 7 (Fig. S6). Another consequence of introgression is that the
215 coalescence time between different subtypes can vary markedly within and across
216 chromosomes, ranging from an estimated 776 to 146,415 generations ago (Table S7).
217 Furthermore, many recombination events are detected in the peri-telomeric genes (Fig. 4a).
218 Interestingly, of the 44 genes that appear to be under positive selection ($K_a/K_s > 1$; see Fig.
219 2a), no less than 17 (38.64%) are affected by recombination. This is significantly higher than
220 the 6.57% of genes (237 out of 3607 genes) affected by recombination that are neutrally
221 evolving or under purifying selection ($K_a/K_s < 1$) (Chi-square test: $X^2 = 54.51$, $df = 1$, $p =$
222 1.55×10^{-13}). In addition, a significantly greater number of recombination events is observed in
223 *C. p. anthroponosum* ($n=39$) than in *C. hominis* ($n=7$) (binomial test: $p = 3.12 \times 10^{-7}$) and *C. p.*
224 *parvum* ($n=17$) (binomial test: $p = 0.011$) (Table S7). These analyses suggest that the genetic
225 exchange between diverged lineages is unlikely to be a neutral process and may be fuelling
226 adaptation in anthroponotic lineages of *Cryptosporidium*.

227

228 Finally, we estimate the divergence dates to provide the first chronological description for
229 genetic introgression between human-infective *Cryptosporidium* spp. (Fig. 4b). The majority
230 of introgression events between *C. p. parvum* and *C. p. anthroponosum* strains are estimated
231 to have taken place at approximately 10-15 thousand generations ago (TGA). Only circa
232 6.8% of all genetic exchanges are introgression events into the *C. hominis* genome, and as
233 expected, these events are more ancient (i.e. ~75-150 TGA). To translate generation time into
234 years and estimate the age of the introgression events, we assume a generation time of
235 between 48 and 96 hours^{24,25}, and a steady rate of transmission within host populations. The
236 following estimates should be considered minimum estimates of divergence times because
237 *Cryptosporidium* may be dormant outside the host. We estimate that the zoonotic *C. p.*
238 *parvum* and the anthroponotic *C. p. anthroponosum* strains are likely to have recombined
239 between 55-164 years ago, whereas we estimate that introgression events between *C. hominis*
240 and *C. parvum* occurred between 410-1096 years ago (Fig. 4b). We show that despite genetic
241 adaptation to specific hosts, diverged *Cryptosporidium* (sub)species continue to exchange
242 genetic information through hybridisation within the last millennium, and that such exchange
243 does not appear to be selectively neutral.

244

245 Discussion

246 *Cryptosporidium* is an apicomplexan parasite that can cause debilitating gastrointestinal
247 illness in animals and humans worldwide. In order to better understand the biology of this
248 parasite, we conducted an analysis to describe the population structuring based on 467
249 sequences of a highly-polymorphic locus (gp60), and we study the evolution of this parasite
250 using 16 whole genome sequences. We demonstrate here that *C. parvum* consists of two
251 subspecies with distinct host associations, namely *C. p. parvum* (zoonotic) and *C. p.*
252 *anthroponosum* (anthroponotic) that have diverged recently. Nevertheless, the population

253 genetic structure differs significantly between both subspecies, with *C. p. parvum* showing a
254 strong isolation-by-distance signal, whilst there is no clear geographic structure for *C. p.*
255 *anthroponosum*. Besides the apparent differences in drift and gene flow, the divergence of
256 both subspecies is also driven by positive selection, and the signature of adaptive evolution is
257 comparable to that of *C. p. parvum* and *C. hominis*. Perhaps most remarkably, hybridisation
258 has frequently led to the genetic introgression between these (sub)species. Given that such
259 exchanges appear to be associated in particular to genes under positive selection, we believe
260 that hybridisation plays an important role throughout the evolution of these parasites. Next,
261 we describe *Cryptosporidium* biology with the aim to interpret and explain the population
262 genetic and evolutionary genetic findings, placing them into the context of recent whole
263 genome studies of other pathogens.

264
265 Our population genetic analysis detected remarkable differences between *C. p.*
266 *anthroponosum* and *C. p. parvum*, both in their population genetic structure, as well as their
267 levels of nucleotide diversity. *C. p. parvum* can cause neonatal enteritis (scour)
268 predominantly in pre-weaned calves²⁶. Given that such calves are able to produce circa
269 100,000 oocysts per gram of faeces, they are thought to be the primary source of subsequent
270 infections²⁷. Movement of such young animals has therefore been highly restricted by the
271 European Union^{28,29}. Adult cattle tend to be asymptomatic and shed fewer oocysts, and
272 consequently, they are believed to be minor transmission vectors. Furthermore, long distance
273 translocation of cattle is rare compared to human migration; just 42,515 cattle were exported
274 to the EU from the UK³⁰ whereas 70.8 million overseas visits were made by UK residents in
275 2016³¹. Consequently, in cattle *C. p. parvum* mediated scour is unlikely to be spread by long
276 distance migration via the livestock trade in Europe. In contrast, a significant component of
277 human cryptosporidiosis is traveller's diarrhoea – and even where contracted domestically,
278 the source of infection is frequently distant^{32,33,34}. We propose that the difference in migration
279 patterns between the primary hosts can explain why we find no evidence of isolation-by-
280 distance for *C. p. anthroponosum* in Europe, whilst there is strong geographic structuring in
281 *C. p. parvum*. Differences in the rate of gene flow can also explain the notable distinction in
282 the nucleotide diversity between these subspecies, which is almost an order of magnitude
283 higher in *C. p. anthroponosum* than in *C. p. parvum*. Interestingly, parasite species from the
284 *Plasmodium* genus show the opposite pattern in that the human-infective parasite species (*P.*
285 *falciparum* and *P. malariae*) have a significantly lower nucleotide diversity compared to
286 related zoonotic malarias (*P. reichenowi* and *P. malariae*-like)^{35,36}. In this example, the lack
287 of diversity in human-infective species has been interpreted as evidence for their recent
288 population expansions. In *C. p. anthroponosum*, however, our population genetic analysis
289 suggests that nucleotide diversity in the European population has been restored by
290 introduction of novel genetic variation through immigration from diverged source
291 populations outside Europe, as well as by genetic introgression.

292
293 Besides gene flow, our analysis identifies a strong signal of hybridisation between diverged
294 strains or species, and we suggest that such genetic exchange between diverged taxa (i.e.
295 genetic introgression) may also have contributed to the rapid restoration of diversity of *C. p.*
296 *anthroponosum*. We detect 104 unique recombination events and estimate that the genetic
297 exchanges have taken place relatively recently, i.e. within the last millennium or ~100,000
298 generations. This implies that hybridisation plays an important role in the biology of
299 *Cryptosporidium*, and that this complex of *Cryptosporidium* species is coevolving in the
300 presence of recent or continued genetic exchange. This interpretation is consistent with the
301 growing body of evidence suggesting that hybridisation of diverged strains plays an
302 important role in pathogen evolution^{6,37}. Hybridisation can lead to the sharing of conserved

303 haploblocks across distinct phylogenetic lineages or (sub)species. Such mosaic-like genomes
304 have been observed also in other human pathogens like *Toxoplasma gondii*⁷, as well some
305 plant pathogens such as the oomycete, *Albugo candida*³⁸. Hybridisation can only occur,
306 however, when different strains are in physical contact with one another. Unlike *A. candida*,
307 which appears to suppress the host's immune response and facilitate coinfections³⁸, challenge
308 experiments with human-infective isolates have shown that different *Cryptosporidium*
309 species compete with each other within the host. For example, the *C. parvum parvum* strain
310 GCH1 (subtype IIa) was shown to rapidly outcompete *C. hominis* strain TU502 (subtype Ia)
311 during mixed infections in piglets³⁹. Nevertheless, mixed species infections or intra-species
312 diversity in *Cryptosporidium* have been identified in a large number (n = 55) of
313 epidemiological surveys of cryptosporidiosis conducted in the period between 2005 – 2015⁴⁰.
314 As with *A. candida*, during the potentially brief periods of coinfections, hybridisation
315 between distinct *Cryptosporidium* lineages may take place within a single host. In turn, this
316 could facilitate the genetic exchange between the diverged lineages and contribute to the
317 (virulence) evolution of *Cryptosporidium*. Introgression from an unidentified source into
318 chromosome 8 of isolate UKP16 illustrates the diversity of the genepool that is able to
319 exchange genetic variation, and it highlights the need for whole genome sequence studies for
320 our understanding of *Cryptosporidium* biology. Interestingly, the distribution of
321 recombination events varies markedly across chromosomes, a pattern observed also in other
322 pathogens such as *T. gondii*⁷. Most remarkably, however, we found that in *Cryptosporidium*
323 genes with a signature of positive selection were significantly more likely to be located in
324 recombination blocks than neutrally evolving genes and genes under purifying selection. Our
325 analyses thus suggest that such exchange is unlikely to be a neutral process, and that the
326 recent emergence of the specialised anthroponotic subspecies such as *C. p. anthroponosum*
327 might be fuelled by relatively recent, and possibly ongoing, "adaptive introgression"³⁷. We
328 estimate that these founding introgression events in the divergence of zoonotic *C. p. parvum*
329 from the anthroponotic *C. p. anthroponosum* began 55-164 years ago, whereas those between
330 *C. hominis* and *C. parvum* occurred between 410-1096 years ago timing which is consistent
331 with reduced livestock contact and increased human population densities – conditions
332 providing a continued selection pressure for the emergence of new human adapted pathogens
333 from zoonotic origins.

334
335

336 **Methods**

337 *Systematic Review*

338 A human cryptosporidiosis prevalence database was constructed using data from peer-
339 reviewed publications retrieved using the search term "Cryptosporidium" from PubMed
340 (<https://www.ncbi.nlm.nih.gov/pubmed>) published between 2000-2017. After filtering (see SI
341 Methods), the final dataset consisted of 743 publications of human *Cryptosporidium*
342 infections in 126 countries.

343 *Empirical Data*

344 Whole genome sequence (WGS) data for *C. hominis* UKH1 and *C. meleagridis* UKMEL 1
345 were retrieved from the *Cryptosporidium* genetics database resource CryptoDB
346 (www.cryptodb.org)⁴¹. The remaining 19 *Cryptosporidium* spp. WGS datasets were
347 obtained from clinical isolates⁸ (see Table S1).

348 *Concatenated Phylogenetic Analysis*

349 61 neutrally-evolving loci ($Ka/Ks = 0.2-0.6$; 93.0-98.0% nucleotide IDs) between *C. parvum*
350 UKP6 and *C. hominis* UKH4 were concatenated. A concatenated approach targeting neutral
351 loci was used in lieu of the well-known gp60 subtyping locus, as this highly recombinant
352 locus frequently produces phylogenies that do not correlate with genome-wide divergence
353 (Fig. S7)⁴². Orthologous protein coding sequences from the human-infective WGS UKP6 and
354 UKH4 were extracted (Table S10), and aligned using ClustalW. The Maximum Likelihood
355 phylogeny was constructed with the Dayhoff substitution model, the Nearest-Neighbour-
356 Interchange method and 2,000 bootstraps⁴³. Divergence statistics between lineages were
357 calculated using MEGA7⁴³.

358 *Whole Genome Comparisons*

359 Parallel whole genome comparative analyses were performed between a zoonotic *C. p.*
360 *parvum* IIAA15G2R1-subtype WGS (UKP6), anthroponotic *C. p. anthroponosum* IIcA5G3a-
361 subtype (UKP15), and anthroponotic *C. hominis* IA14R3-subtype (UKH4). CDS nucleotide
362 divergence was evaluated by cross-blasting CDS datasets locally (BLOSUM62 substitution
363 matrix; BioEdit)⁴⁴. Amino acid identities and indels resulting in frameshift were identified
364 using EMBOSS Stretcher⁴⁵. Selection was identified by calculating Ka/Ks in CodeML of
365 PAML⁴⁶, and NaturalSelection.jl (<https://github.com/BioJulia/NaturalSelection.jl>). Sliding
366 window Ka/Ks analyses, indel characterisations, and F_{ST} calculations were performed in
367 DnaSP 5.10.1⁴⁷. Putative protein function was evaluated using the UniProt BLASTp function
368 (cut-off E-value $<10e-5$)⁴⁸, and putative protein localization was estimated using WoLF
369 PSORT⁴⁹.

370 *Phylogenomic analysis*

371 Sequence reads of 21 *Cryptosporidium* isolates (Table S1) were aligned to the *C. parvum*
372 Iowa⁹ reference genome and SNPs identified (see SI Methods). Pseudoreferences were
373 generated with filtered biallelic SNPs inserted using GATK FastaAlternateReferenceMaker⁵⁰.
374 Principle component analysis of *C. p. parvum* and *C. p. anthroponosum* isolates was
375 performed with SNPrelate⁵¹. Population genetic statistics the fixation index (F_{ST}), absolute
376 divergence (d_{xy}) and nucleotide diversity (π) were estimated in 50 Kb sliding windows (10
377 Kb step size) across the genome. Maximum likelihood phylogenies were estimated for 50
378 SNP windows across the genome using RAxML⁵². Topology weighting²³ was used to
379 investigate the distribution of phylogenetic relationships across the genome with each isolate
380 assigned to one of four groups (*C. p. parvum*, *C. p. anthroponosum*, UKP16 and outgroup
381 samples (*C. hominis* and *C. cuniculus*). Ultrametric phylogenetic trees were made using the
382 *chronopl* function in APE⁵³, and a consensus phylogeny was generated.

383 *Recombination Analysis*

384 Recombination signals due to introgression were detected using RDP4⁵⁴. Automated
385 detection algorithms RDP, GENECONV, Bootscan, Maxchi, and Chimaera were run with
386 default values. Alternative call (AC) values of all bases in the four isolates that were studied
387 in the genetic introgression analysis (UKH1, UKP6, UKP15 and UKP16) to validate that they
388 comprised single subtype infections (Fig. S8).

389 *Dating introgression events*

390 Hybridization dating was estimated for introgressed regions in HybridCheck⁵⁵. The HKY85
391 substitution model with a SNP mutation rate of $\mu=10^{-8}$ per generation was assumed, based on
392 the observed nucleotide divergence between two outbreak WGS sampled seven days apart
393 (Table S8). To convert generations into time, we assumed a factor of 12 autoinfective
394 offspring per parental oocyst *in vivo* (Fig. S9). Furthermore, past infectivity studies revealed a
395 population expansion of 3-5 new generations, and an estimated life cycle duration of 48-96h
396 per infection (Table S9)^{60,61}. This estimate is longer than previous estimates (12-14h)⁵⁶, but
397 consistent with estimates of 72h from a cell culture experiment⁵⁷. The reported estimates of
398 time may be underestimated if oocysts remain dormant in the environment between infections
399 of different host individuals.

400 *Population Genetic Analysis*

401 A total of 467 gp60 sequences collected in 43 countries were used to analyse the population
402 structure of *C. p. parvum* UKP6 (N=361) and *C. p. anthroponosum* UKP15 (N=106) (see SI
403 Methods). Population genetic structure was visualised using Fluxus network using median
404 joining setting⁵⁸. Isolation-by-distance analysis was performed using a regression analysis of
405 the genetic distance (Kxy) between isolates and geographic distance between the sampling
406 locations. Differences between chromosomes, chromosomal regions, recombinant regions
407 and genes in the number of SNPs, indels, and recombination events were tested with Chi-
408 square and binomial tests. Differences in nucleotide substitution patterns, indels and
409 recombination events between taxa were analysed using Mann-Whitney test and ANOVAs.
410 All tests were conducted in R (R Core Team)⁵⁹ and Minitab 12.1.

412 *Data availability*

413 All WGS data used in this paper is available publically and for free via the NCBI server
414 (<https://www.ncbi.nlm.nih.gov/>) or CryptoDB (<http://cryptodb.org/cryptodb/>). The accession
415 codes for the data are provided in Table S1.

416

417

418 **Author's contributions**

419 KT, RC, PH, JN and CvO conceived the study. JN and CvO designed the analyses. JN, JP, GR, MS, PH, KT
420 and RC were involved in the acquisition of data. JN conducted the meta-analysis. JN and CvO conducted the
421 evolutionary genetic analyses with input of TM for the phylogenetic and BW for the recombinant analyses. JN
422 and CvO drafted the submitted manuscript. All authors contributed to revising the draft, had full access to all the
423 data and read and approved the final manuscript.

424

425 **Acknowledgements**

426 This work was supported with funds awarded to KT and RMC from the FP7 KBBE EU project
427 AQUAVALENS, grant agreement 311846 from the European Union awarded to PH, and a Biotechnology and
428 Biological Sciences Research Council (BBSRC) (BB/N02317X/1) awarded to CvO, as well as support by the
429 Earth & Life Systems Alliance (ELSA). P.R.H. is supported by the National Institute for Health Research
430 Health Protection Research Unit (NIHR HPRU) in Gastrointestinal Infections at the University of Liverpool, in
431 partnership with Public Health England (PHE), and in collaboration with University of East Anglia, University
432 of Oxford, and the Institute of Food Research. Professor Hunter is based at the University of East Anglia. The
433 views expressed are those of the authors and not necessarily those of the National Health Service, the National
434 Institute for Health Research, the Department of Health, or Public Health England. We thank Gregorio Pérez-
435 Córdona for VNTR validation of isolates, and we thank the three reviewers for their helpful comments.

436

437 **Competing Interests**

438 The authors declare that there is no conflict of interest regarding the publication of this article.

439

440 **References**

441

442 ¹Liu, L. *et al.* Global, regional, and national causes of child mortality: an updated systematic
443 analysis for 2010 with time trends since 2000. *Lancet* **379**, 2151-2161 (2012).

444 ²Kotloff, K. L. *et al.* Burden and aetiology of diarrhoeal disease in infants and young children
445 in developing countries (the Global Enteric Multicenter Study, GEMS): a prospective, case-
446 control study. *Lancet* **382**, 209-222 (2013).

447 ³Widmer, G., & Sullivan, S. Genomics and population biology of *Cryptosporidium* species.
448 *Parasite Immunol.* **34**, 61-71 (2012).

449 ⁴Mazurie, A. *et al.* Comparative genomics of *Cryptosporidium*. *Int. J. Genomics* **2013**,
450 832756 (2013).

451 ⁵Bushell, E. *et al.* Functional profiling of a *Plasmodium* genome reveals an abundance of
452 essential genes. *Cell* **170**, 260-72 (2017).

453 ⁶McMullan, M. *et al.* Evidence for suppression of immunity as a driver for genomic
454 introgressions and host range expansion in races of *Albugo candida*, a generalist parasite.
455 *eLife* **4** (2015).

456 ⁷Lorenzi, H. *et al.* Local admixture of amplified and diversified secreted pathogenesis
457 determinants shapes mosaic *Toxoplasma gondii* genomes. *Nature Commun.* **7**, 10147 (2016).

458 ⁸Hadfield, S. J. *et al.* Generation of whole genome sequences of new *Cryptosporidium*
459 *hominis* and *Cryptosporidium parvum* isolates directly from stool samples. *BMC Genomics*
460 **16**, 1-12 (2015).

461 ⁹Abrahamsen, M. S. *et al.* Complete genome sequence of the apicomplexan, *Cryptosporidium*
462 *parvum*. *Science* **304**, 441-445 (2004).

463 ¹⁰Xu, P. *et al.* The genome of *Cryptosporidium hominis*. *Nature* **431**, 1107-1112 (2004).

464 ¹¹Bouzid, M., Hunter, P. R., Chalmers, R. M., & Tyler, K. M. *Cryptosporidium* pathogenicity
465 and virulence. *Clin. Microbiol. Rev.* **26**, 115-134 (2013).

466 ¹²Widmer, G. *et al.* Comparative genome analysis of two *Cryptosporidium parvum* isolates
467 with different host range. *Infect. Genet. Evol.* **12**, 1213-1221 (2012).

468 ¹³Guo, Y. *et al.* Comparative genomic analysis reveals occurrence of genetic recombination
469 in virulent *Cryptosporidium hominis* subtypes and telomeric gene duplications in
470 *Cryptosporidium parvum*. *BMC Genomics* **16**, 1-18 (2015).

471 ¹⁴Li, N. *et al.* Genetic recombination and *Cryptosporidium hominis* virulent subtype
472 IbA10G2. *Emerg. Infect. Dis.* **19**, 1573-82 (2013).

473 ¹⁵Xiao, L. & Ryan U. M. Cryptosporidiosis: an update in molecular epidemiology. *Curr.*
474 *Opin. Infect. Dis.* **17**, 483-90 (2004).

475 ¹⁶Puleston, R. L. *et al.* The first recorded outbreak of cryptosporidiosis due to
476 *Cryptosporidium cuniculus* (formerly rabbit genotype), following a water quality incident. *J.*
477 *Water Health* **12**, 41-50 (2014).

478 ¹⁷Koehler, A. V., Whipp, M. J., Haydon, S. R. & Gasser, R. B. *Cryptosporidium cuniculus* -
479 new records in human and kangaroo in Australia. *Parasit. Vectors* **7**, 492 (2014).

480 ¹⁸Wang, Y. *et al.* Population genetics of *Cryptosporidium meleagridis* in humans and birds:
481 evidence for cross-species transmission. *Int. J. Parasitol.* **44**, 515-21 (2014).

482 ¹⁹Koehler, A. V. *et al.* *Cryptosporidium viatorum* from the native Australian swamp rat
483 *Rattus lutreolus* - An emerging zoonotic pathogen? *Int. J. Parasitol. Parasites Wildl.* **7**, 18-26
484 (2018).

485 ²⁰Li, N. *et al.* Subtyping *Cryptosporidium ubiquitum*, a zoonotic pathogen emerging in
486 humans. *Emerg. Infect. Dis.* **20**, 217-24 (2014).

487 ²¹Joachim, A. Human cryptosporidiosis: an update with special emphasis on the situation in
488 Europe. *J. Vet. Med. B Infect. Dis. Vet. Public Health* **51**, 251-9. (2004).

489 ²²Chappell, C. L. *et al.* *Cryptosporidium muris*: infectivity and illness in healthy adult
490 volunteers. *Am. J. Trop. Med. Hyg.* **92**, 50-5 (2015).

491 ²³Martin, S. H. & Van Belleghem, S. M. Exploring evolutionary relationships across the
492 genome using topology weighting. *Genetics* **206**, 429-438 (2017).

493 ²⁴Okhuysen, P. C. *et al.* Infectivity of a *Cryptosporidium parvum* isolate of cervine origin for
494 healthy adults and interferon-gamma knockout mice. *J. Infect. Dis.* **185**, 1320-5 (2002).

495 ²⁵Chappell, C. L. *et al.* *Cryptosporidium meleagridis*: infectivity in healthy adult volunteers.
496 *Am. J. Trop. Med. Hyg.* **85**, 238-42 (2011).

497 ²⁶Santín, M., Trout, J. M., & Fayer, R. A longitudinal study of cryptosporidiosis in dairy
498 cattle from birth to 2 years of age. *Vet. Parasitol.* **155**, 15-23 (2008).

499 ²⁷Current, W. L. Cryptosporidiosis. *J. Am. Vet. Med. Assoc.* **187**, 1334-8 (1985).

500 ²⁸Animal Transport Guides, Transport of calves. (2017). at:
501 <<http://animaltransportguides.eu/>>.

502 ²⁹Defra., PB 12544a: Welfare of Animals During Transport. (2011).

503 ³⁰LAres, E., & Ward, M. Live animal exports. *Commons Library Briefing.* **8031** (2017).

504 ³¹ONS. Travel Trends: 2016. (2017).
505 <<https://www.ons.gov.uk/peoplepopulationandcommunity/leisureandtourism/articles/traveltrends/2016>>.
506

507 ³²Jelinek, T. *et al.* Prevalence of infection with *Cryptosporidium parvum* and *Cyclospora*
508 *cayetanensis* among international travellers. *Gut* **41**, 801-804 (1997).

509 ³³Nair, P. *et al.* Epidemiology of cryptosporidiosis in North American travelers to Mexico.
510 *Am. J. Trop. Med. Hyg.* **79**, 210-4 (2008).

511 ³⁴Chalmers, R. M. *et al.* Geographic linkage and variation in *Cryptosporidium hominis*.
512 *Emerg. Infect. Dis.* **14**, 496-8 (2008).

513 ³⁵Sundararaman, S. A. *et al.* Genomes of cryptic chimpanzee *Plasmodium* species reveal key
514 evolutionary events leading to human malaria. *Nat. Commun.* **22**, 11078 (2016).

515 ³⁶Rutledge, G. G. *et al.* *Plasmodium malariae* and *P. ovale* genomes provide insights into
516 malaria parasite evolution. *Nature* **542**, 101-104 (2017).

517 ³⁷King, K. C., Stelkens, R. B., Webster, J. P., Smith, D. F. & Brockhurst, M. A.
518 Hybridization in parasites: consequences for adaptive evolution, pathogenesis, and public
519 health in a changing world. *PLoS Pathog.* **11** (2015).

520 ³⁸Jouet, A. *et al.* *Albugo candida* race diversity, ploidy and host-associated microbes
521 revealed using DNA sequence capture on diseased plants in the field. *New Phytol.*
522 doi: [10.1111/nph.15417](https://doi.org/10.1111/nph.15417) (2018).

523 ³⁹Akiyoshi, D. E., Mor, S. & Tzipori, S. Rapid displacement of *Cryptosporidium parvum* type
524 1 by type 2 in mixed infections in piglets. *Infect. Immun.* **71**, 5765-71 (2003).

525 ⁴⁰Grinberg, A. & Widmer, G. *Cryptosporidium* within-host genetic diversity: systematic
526 bibliographical search and narrative overview. *Int. J. Parasitol.* **46**, 465-71 (2016).

527 ⁴¹Puiu, D. *et al.* CryptoDB: the *Cryptosporidium* genome resource. *Nucleic Acids Res.* **32**,
528 D329-31 (2004).

529 ⁴²Feng, Y., Ryan, U. M. & Xiao, L. Genetic diversity and population structure of
530 *Cryptosporidium*. *Trends Parasitol.* **34**, 997-1011 (2018).

531 ⁴³Kumar, S., Stecher, G. & Tamura, K. MEGA7: Molecular Evolutionary Genetics Analysis
532 Version 7.0 for Bigger Datasets. *Mol. Biol. Evol.* **33**, 1870-4 (2016).

533 ⁴⁴Hall, T. A. BioEdit: a user-friendly biological sequence alignment editor and analysis
534 program for Windows 95/98/NT. *Nucleic Acids Symposium Series* **41**, 95-98 (1999).

535 ⁴⁵Rice, P., Longden, I. & Bleasby, A. EMBOSS: the European Molecular Biology Open
536 Software Suite. *Trends Genet.* **16**, 276-7 (2000).

537 ⁴⁶Suyama, M., Torrents, D. & Bork P. PAL2NAL: robust conversion of protein sequence
538 alignments into the corresponding codon alignments. *Nucleic Acids Res.* **34**, W609-12
539 (2006).

540 ⁴⁷Librado, P. & Rozas, J. DnaSP v5: a software for comprehensive analysis of DNA
541 polymorphism data. *Bioinformatics* **25**, 1451-2 (2009).

542 ⁴⁸Apweiler, R. *et al.* UniProt: the Universal Protein knowledgebase. *Nucleic Acids Res.* **32**,
543 D115-9 (2004).

544 ⁴⁹Horton, P. *et al.* WoLF PSORT: protein localization predictor. *Nucleic Acids Res.* **35**,
545 W585-7 (2007).

546 ⁵⁰DePristo, M. A. *et al.* A framework for variation discovery and genotyping using next-
547 generation DNA sequencing data. *Nature Genet.* **43**, 491-8 (2011).

548 ⁵¹Zheng, X. *et al.* A High-performance Computing Toolset for Relatedness and Principal
549 Component Analysis of SNP Data. *Bioinformatics* **28**, 3326-3328 (2012).

550 ⁵²Stamatakis, A. RAxML version 8: a tool for phylogenetic analysis and post-analysis of
551 large phylogenies. *Bioinformatics* **30**, 1312-3 (2014).

552 ⁵³Paradis, E., Claude, J. & Strimmer, K. APE: Analyses of Phylogenetics and Evolution in R
553 language. *Bioinformatics* **20**, 289-90 (2004).

554 ⁵⁴Martin, D. P., Murrell, B., Golden, M., Khoosal, A. & Muhire, B. RDP4: Detection and
555 analysis of recombination patterns in virus genomes. *Virus Evol.* **1**, vev003 (2015).

556 ⁵⁵Ward, B. J. & van Oosterhout, C. HYBRIDCHECK: software for the rapid detection,
557 visualization and dating of recombinant regions in genome sequence data. *Mol. Ecol. Resour.*
558 **16**, 534-9 (2016).

559 ⁵⁶Fleming, R. *Cryptosporidium: Could It Be in Your Water?* Ontario Ministry of Agriculture,
560 Food, and Rural Affairs (2015).

561 ⁵⁷Current, W. L. & Haynes, T. B. Complete development of *Cryptosporidium* in cell culture.
562 *Science* **224**, 604-5 (1984).

563 ⁵⁸Bandelt, H. J., Forster, P. & Rohl, A. Median-joining networks for inferring intraspecific
564 phylogenies. *Mol. Biol. Evol.* **16**, 37-48 (1999).

565 ⁵⁹R Core Team. R: A language and environment for statistical computing. R Foundation for
566 Statistical Computing, Vienna, Austria (2013). URL <http://www.R-project.org/>.

567 ⁶⁰Kosek, M., Alcantara, C., Lima, A. A. & Guerrant, R. L. Cryptosporidiosis: an update.
568 *Lancet Infect. Dis.* **1**, 262-9 (2001).

569 ⁶¹O'Hara, S. P. & Chen, X. M. The cell biology of *Cryptosporidium* infection. *Microbes*
570 *Infect.* **13**, 721-30 (2011).

571

572

573 **Legends to Figures**

574

575 **Figure 1**

576 **a**, Concatenated phylogeny of 16 human-infective *Cryptosporidium* spp. The maximum
577 likelihood phylogeny is based on a 142,452 bp alignment of 61 loci (Table S10) and 2,000
578 bootstrap replications. Unique UK-identifiers show species group, specific gp60 subtype, and
579 prevalent host type(s) (Table S1, Fig. S1). **b,c**, Relative global distribution of human
580 cryptosporidiosis due to *C. parvum* (orange) versus *C. hominis* (blue) based on a systematic
581 review of 743 peer-reviewed publications ([Dropbox](#)). Relative proportion of global *C.*
582 *parvum* human cryptosporidiosis due to zoonotic *C. p. parvum* IIa (green) versus
583 anthroponotic *C. p. anthroponosum* IIc-a (purple) based on a systematic review of 84 peer-
584 reviewed publications. **d**, Nucleotide diversity (π) within European *C. p. parvum* (IIa) (green,
585 n=96; Min=0.000000, 1st Qu.=0.001374, Median=0.002762, Mean=0.003244, 3rd
586 Qu.=0.004169, Max=0.006970) and *C. p. anthroponosum* (IIc-a) (purple, n=22;
587 Min=0.000000, 1st Qu.=0.002124, Median=0.043951, Mean=0.029704, 3rd Qu.=0.046250,
588 Max=0.061045) populations. **e**, The genetic distance (Kxy) between *C. p. parvum* (n=345)
589 isolates is strongly correlated with geographic distance (Regression $F_{1,26}=40.63$,
590 $p=0.000000944$, $R^2=61.0\%$), whilst there is no isolation-by-distance signal detected for *C. p.*
591 *anthroponosum* (n=106) isolates ($F_{1,16}=1.477$, $p=0.242$). **f**, *C. p. parvum* (IIa) isolates show
592 an isolation-by-distance signal, as is illustrated by the positive slope of the regression line
593 between genetic differentiation (Fst) and geographic distance (Regression: R^2 -adj.=58.3%,
594 $F_{1,8}=13.60$, $p=0.006$). This signal suggests there is some gene flow within Europe. No
595 isolation-by-distance was found for *C. p. anthroponosum* (IIc-a) in Europe. Combined with
596 significantly higher nucleotide diversity, this suggests that *C. p. anthroponosum* infections
597 arrive from outside Europe, rather than being transmitted within Europe. **g,h**, Fluxus network
598 of global *C. p. parvum* (IIa) and *C. p. anthroponosum* (IIc-a) GenBank-submitted gp60
599 sequences show significant sub-structuring of global populations of *C. p. parvum* IIa isolates,
600 and absence of structure between or within regional populations of *C. p. anthroponosum* IIc-
601 a.

602

603

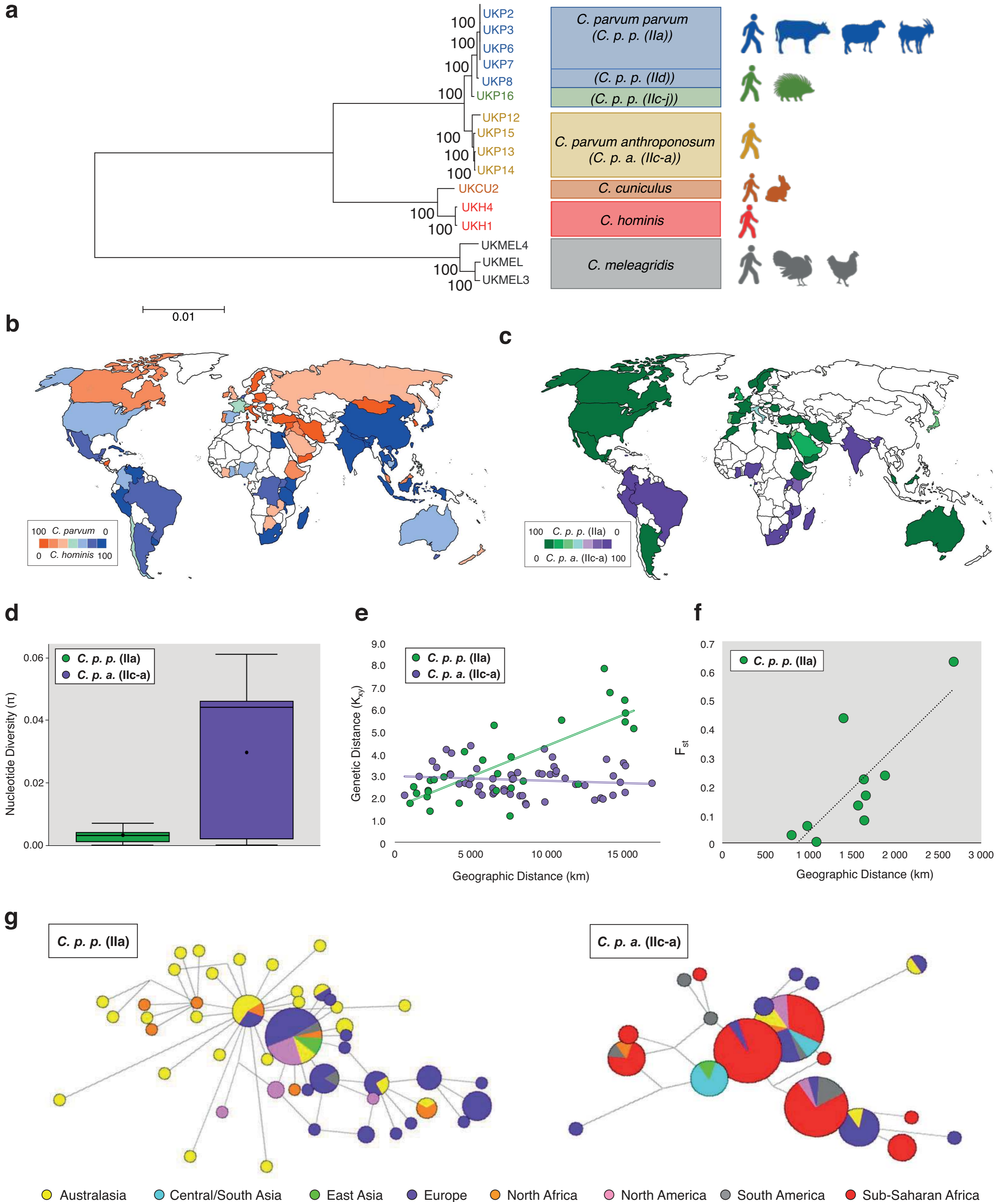
604

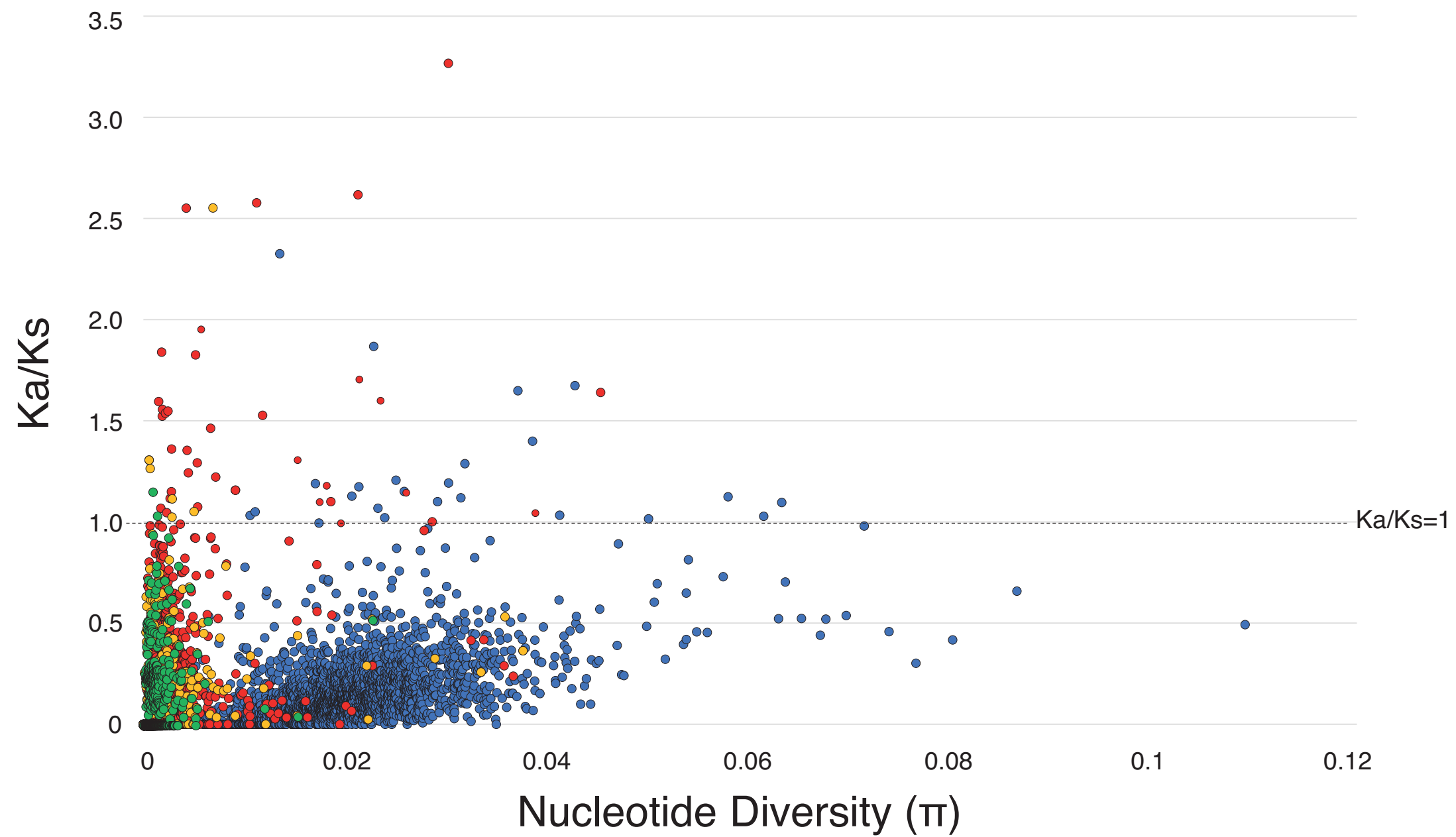
605 **Figure 2**
606 **a,b**, Selective pressures (Ka/Ks) and nucleotide distances (π) generated gene-by-gene
607 between and within zoonotic and anthroponotic *Cryptosporidium* species groups. Zoonotic *C.*
608 *p. parvum* UKP6 genomics coding sequences (CDSs) are here compared to zoonotic *C. p.*
609 *parvum* UKP8 (green; Min=0.00000, 1st Qu.=0.00000, Median=0.00000, Mean=0.1613, 3rd
610 Qu.=0.00000, Max=1.00000), anthroponotic *C. parvum parvum* UKP16 (yellow;
611 Min=0.00000, 1st Qu.=0.00000, Median=0.00000, Mean=0.17991, 3rd Qu.=0.09046,
612 Max=1.00000), anthroponotic *C. p. anthroponosum* UKP15 (red; Min=0.00000, 1st Qu.=
613 0.00000, Median=0.00000, Mean=0.2169, 3rd Qu.=0.2219, Max=1.00000), and
614 anthroponotic *C. hominis* UKH4 (blue; Min=0.00000, 1st Qu.=0.05924, Median=0.11785,
615 Mean=0.13858, 3rd Qu.=0.18854, Max=1.00000). Distribution of global Ka/(Ka+Ks) values
616 for each comparison are shown, and differences were assessed statistically (One-way
617 ANOVA, $F_{12,727} = 31.34$, $P < 3.567e-20$, $n = 3465$ CDSs). **c**, Sliding window analysis of triplet
618 (brown) and non-triplet (green) insertion and deletion (indel) events between two samples,
619 i.e. *C. parvum parvum* UKP6 and *C. parvum anthroponosum* UKP15. Composite results for
620 20 kb-wide sliding windows across chromosomes 1, 2, 4, 6, and 8 are shown. Peri-telomeric
621 genes (T) and subtelomeric genes (S) have significantly more triplet and non-triplet indels
622 than non-telomeric (NT) genes (Chi-sq. test, $X^2 = 38.535$, $df = 2$, $p = 4.29 \times 10^{-9}$; $X^2 = 226.078$,
623 $df = 2$, $p = 8.09e^{-50}$, respectively). **d**, Comparative selective pressure analysis between *C. p.*
624 *parvum* UKP6 and *C. p. anthroponosum* UKP15 coding sequences with contrasting protein
625 localizations. The range of Ka/(Ka+Ks) between all ($n = 3465$; Min=0.00000, 1st
626 Qu.=0.00000, Median=0.1416, Mean=0.3058, 3rd Qu.=0.3989, Max=1.00000) CDSs, CDSs
627 annotated as having a cytoplasmic protein localization ($n = 1152$; Min=0.00000, 1st
628 Qu.=0.00000, Median=0.1110, Mean=0.2980, 3rd Qu.=0.3705, Max=1.00000), and CDSs
629 annotated as having an extracellular localization ($n = 333$; Min=0.00000, 1st Qu.=0.00000,
630 Median=0.1973, Mean=0.4180, 3rd Qu.= 1.00000, Max=1.00000) are represented by a violin
631 plot. CDSs with extracellular localisation experience significantly more positive selection
632 than cytoplasmic CDSs, as evidenced by their higher Ka/(Ka+Ks) value (two-sided Mann-
633 Whitney test, $W = 842985$, $p = 0.0182$). In addition, 17 out of 333 (5.1%) extracellular CDSs
634 have a Ka/Ks larger than unity, compared to just 21 out of 3236 (0.6%) cytoplasmic
635 CDSs (Chi-sq. test: $X^2 = 53.8$, $d.f. = 1$, $p = 1.675e-12$).
636
637
638
639
640

641 **Figure 3**
642 **a**, Principle component analysis of *C. p. parvum* and *C. p. anthroponosum* isolates based on
643 1,476 high quality SNPs retained after pruning based on linkage disequilibrium. **b**, A
644 “cloudogram” of 1,324 trees showing phylogenomic relationships between WGS of
645 anthroponotic *Cryptosporidium* isolates. Maximum likelihood trees were estimated for non-
646 overlapping 50 SNP genomic windows across the *C. parvum* Iowa II reference genome
647 (grey). The consensus phylogeny is shown in black. Isolates belonging to *C. p. parvum* and
648 *C. p. anthroponosum* sub-species fall into two monophyletic groups, *C. hominis*/*C. cuniculus*
649 isolates are included as an outgroup (OG). **c**, Topology weighting was used to explore the
650 genome-wide distribution of phylogenetic relationships between the two *C. parvum*
651 subspecies, a putatively introgressed isolate (UKP16) and an outgroup (*C. hominis* isolates
652 and a single *C. cuniculus* isolate) using the 50 SNP fixed window trees. All possible
653 topologies of the ingroup taxa are shown in the top panel, the lower panel shows the genome-
654 wide average weighting of each topology. **d**, The distribution of topology weightings across
655 chromosome 8 (colours as per c) reveals a putatively introgressed region between 500Kb and
656 650Kb. **e**, Absolute divergence (d_{xy}) between *Cryptosporidium* sub-species and the putatively
657 introgressed isolate UKP16 in 50 Kb sliding windows (10Kb step size) across chromosome 8
658 of the *C. parvum* Iowa II reference genome.
659
660
661

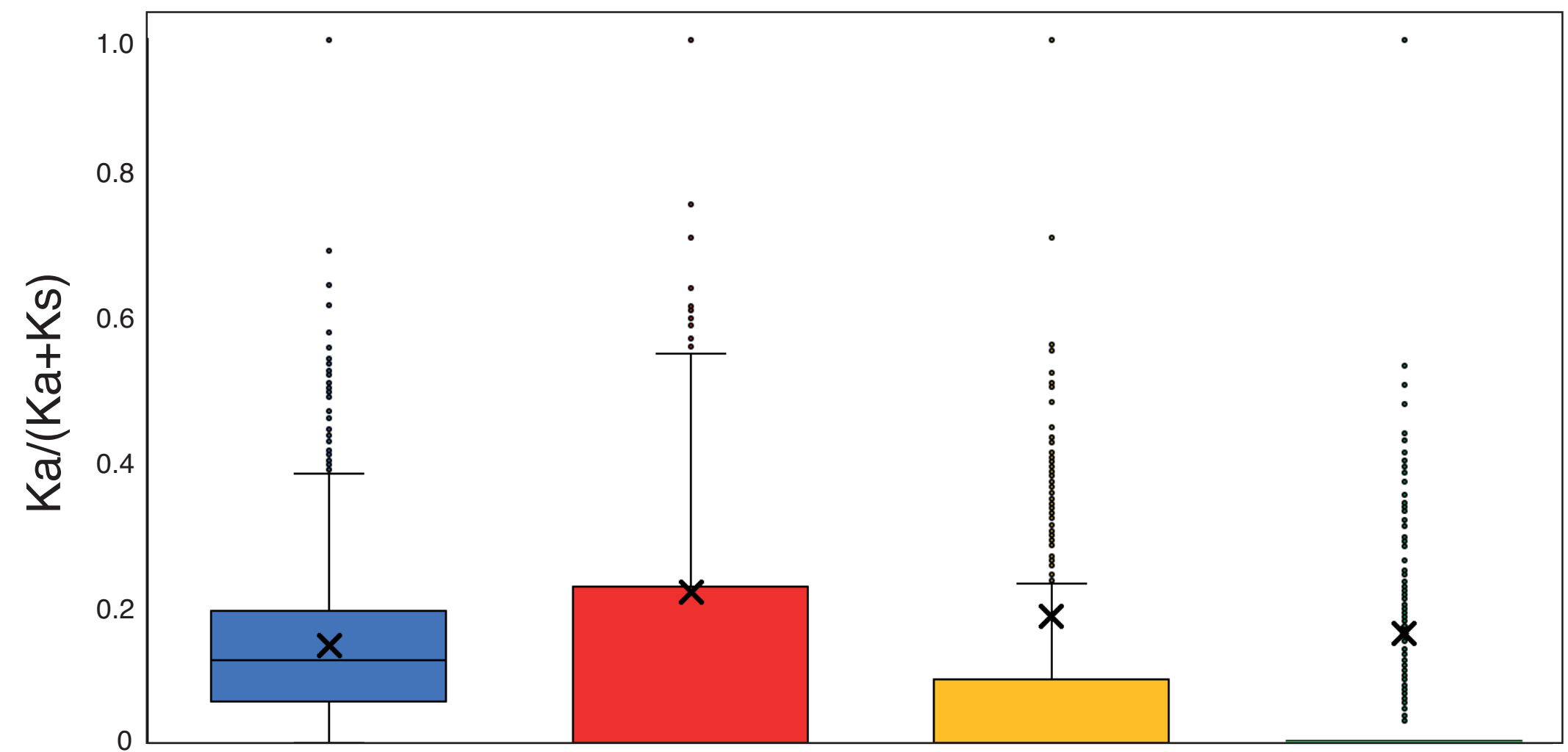
662 **Figure 4**

663 **a**, Genomic recombinant events in anthroponotic *Cryptosporidium spp.* WGS. Size and
664 location of recombinant fragments detected by RDP4 are illustrated for recombination
665 between *C. p. parvum* UKP6 and *C. p. parvum* UKP16 (yellow), *C. p. parvum* UKP6 and *C.*
666 *p. anthroponosum* UKP15 (pink), *C. p. parvum* UKP16 and *C. p. anthroponosum* UKP15
667 (turquoise), *C. p. parvum* UKP6 and *C. hominis* UKH1 (green), *C. p. anthroponosum* UKP15
668 and *C. hominis* UKH1 (blue), and *C. p. parvum* UKP16 and *C. hominis* UKH1 (peach).
669 Recombination events with unknown major or minor parentage are additionally represented
670 (grey). Individual recombination events are detailed in Table S7. **b**, Estimated dates of
671 introgression events between anthroponotic and zoonotic *Cryptosporidium spp.*. The range of
672 estimated introgression times (thousands of generations ago) are given for introgression
673 events between zoonotic *C. p. parvum* (UKP6) and anthroponotic *C. p. anthroponosum*
674 (UKP15) – n=45, Min=7369, 1st Qu.=9218, Median=11486, 3rd Qu=13045, Max=17914 , and
675 for introgression events between zoonotic *C. p. parvum* (UKP6) and anthroponotic *C.*
676 *hominis* (UKH1) – n=33, Min=64655, 1st Qu.=77337, Median=95974, Mean=103281, 3rd
677 Qu.117130, Max=188341. Minimum, mean, and maximum generation numbers were
678 converted into units of time (years) for both 48- and 96-hour life cycle estimates.

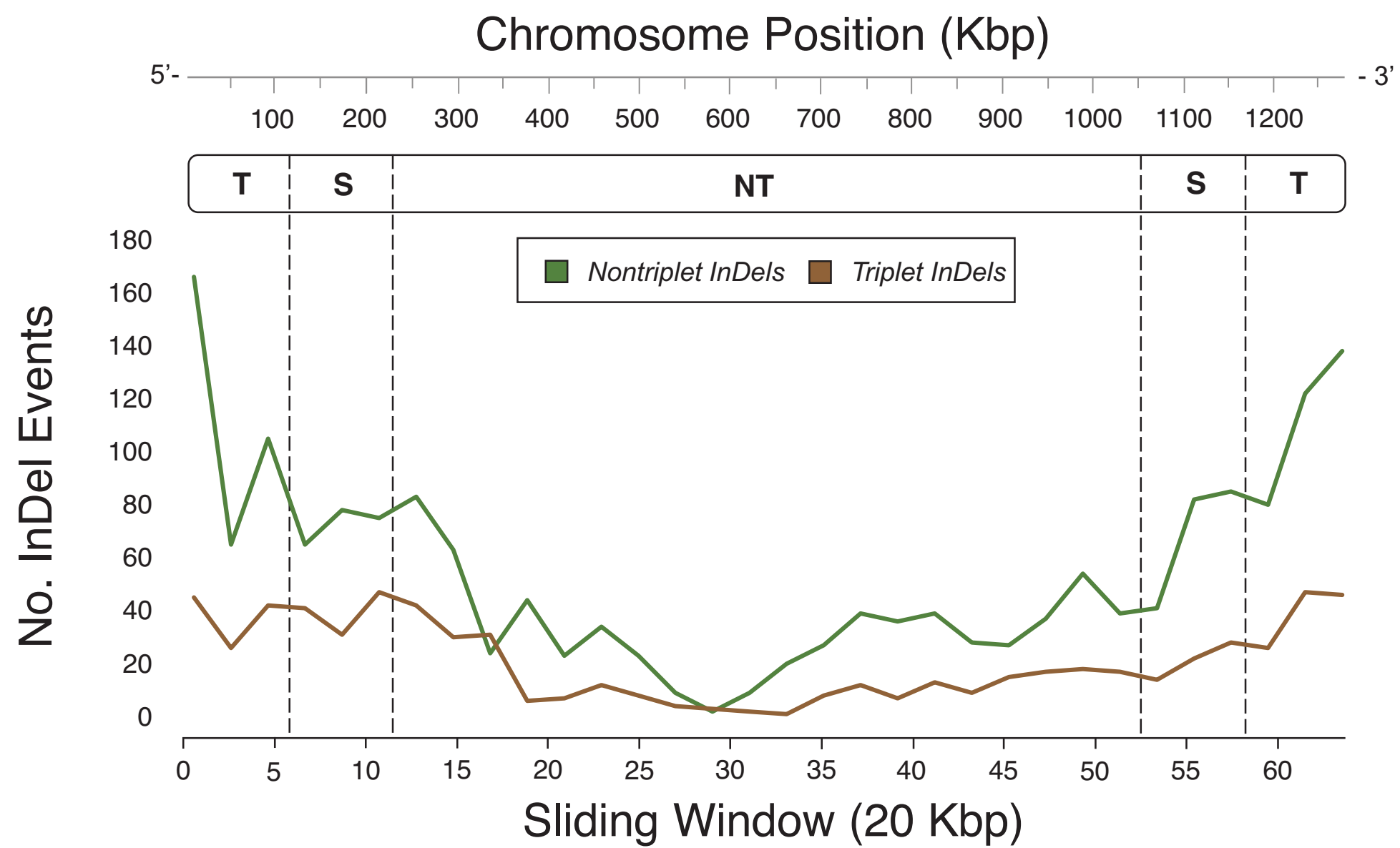
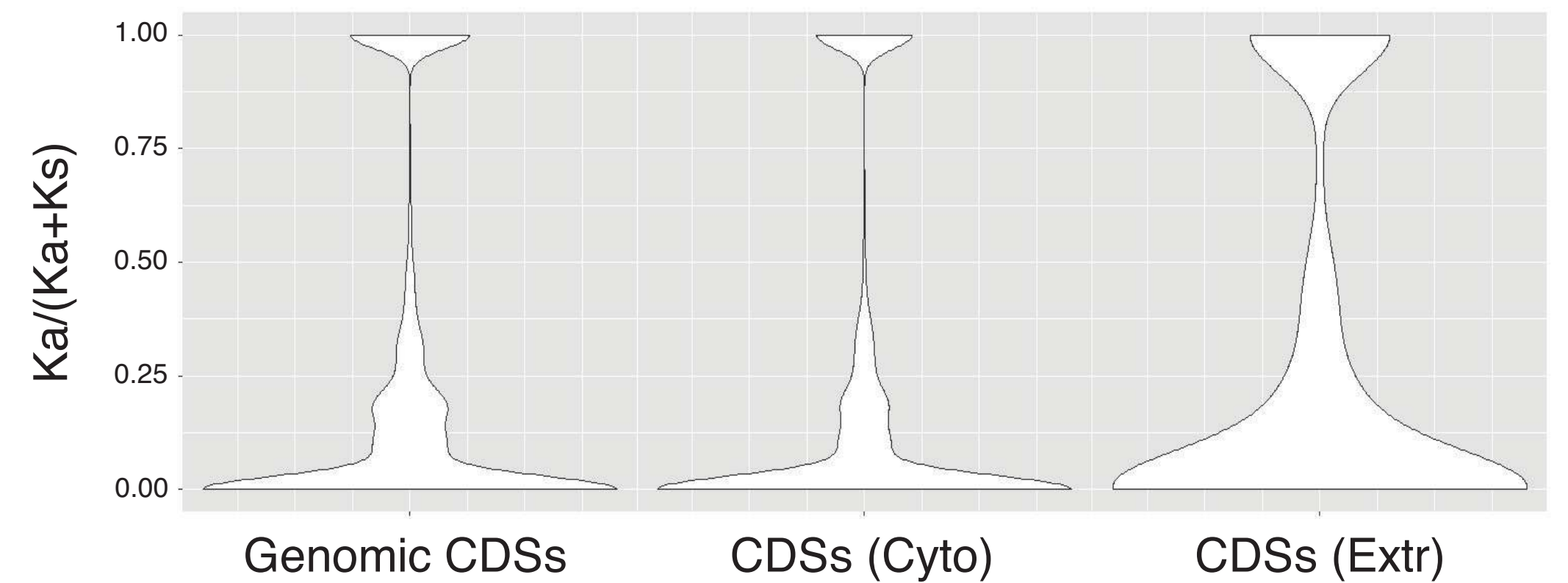


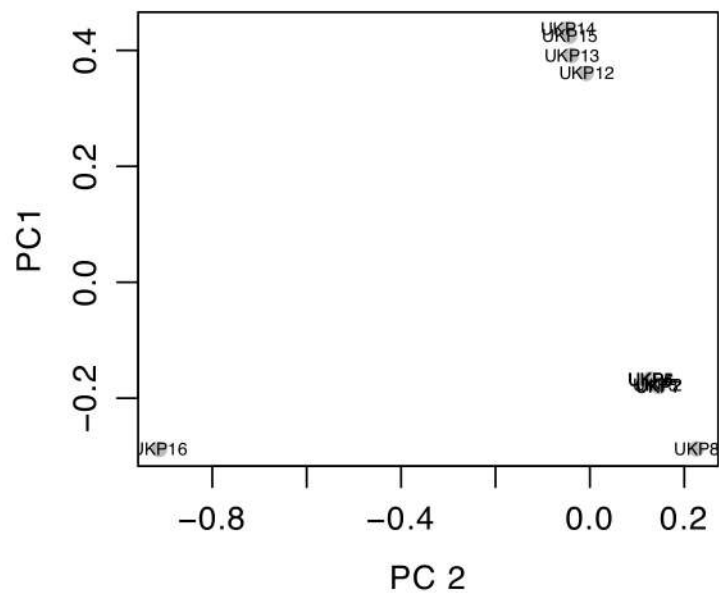
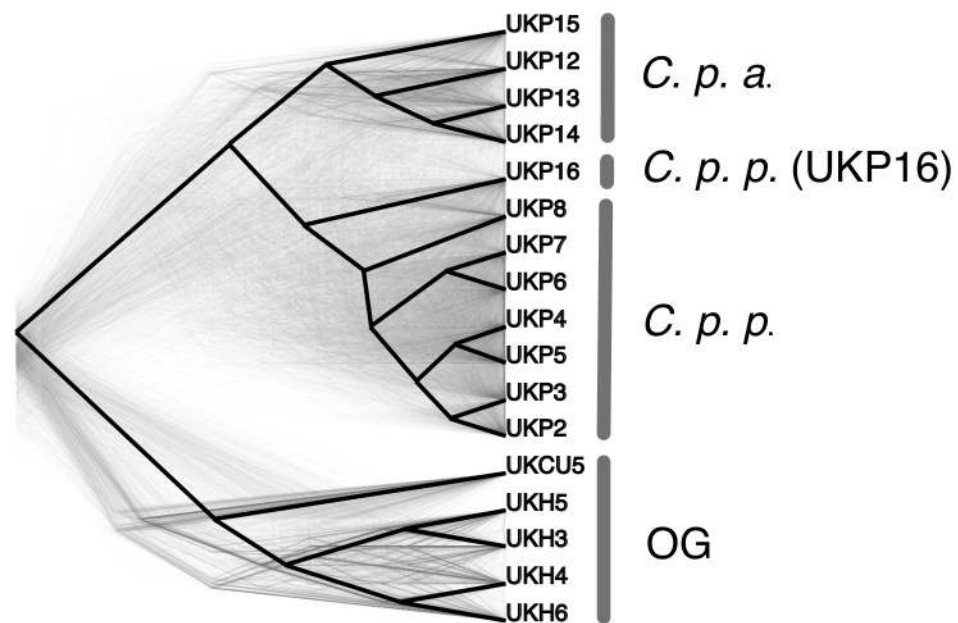
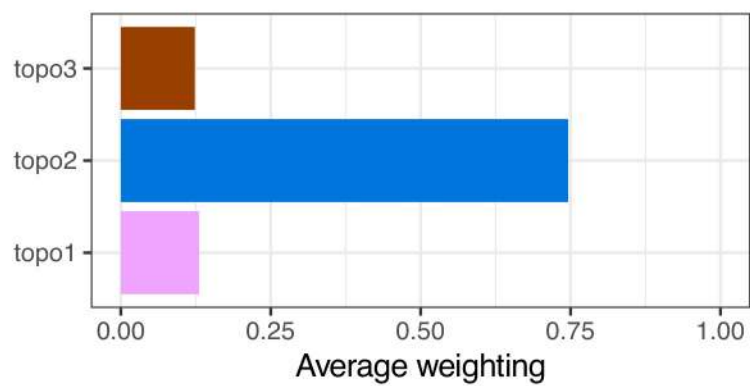
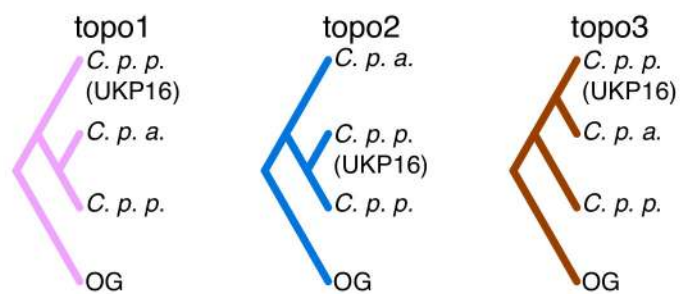
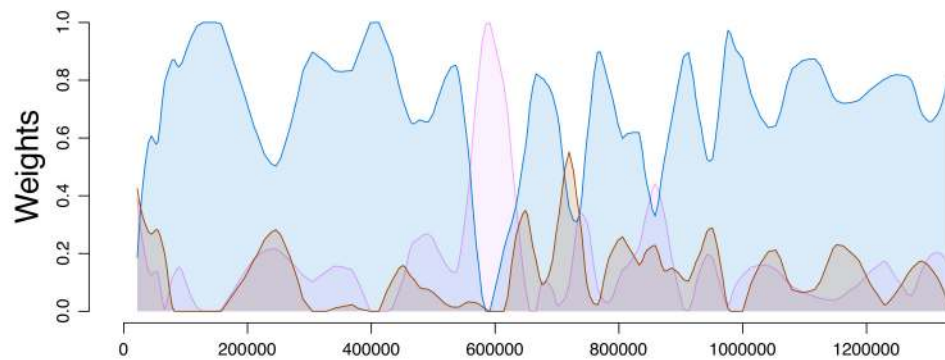
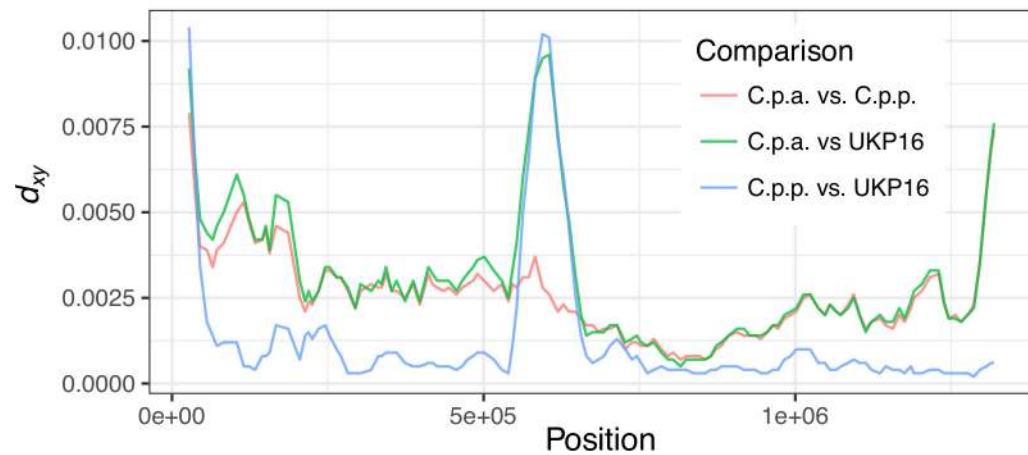
a

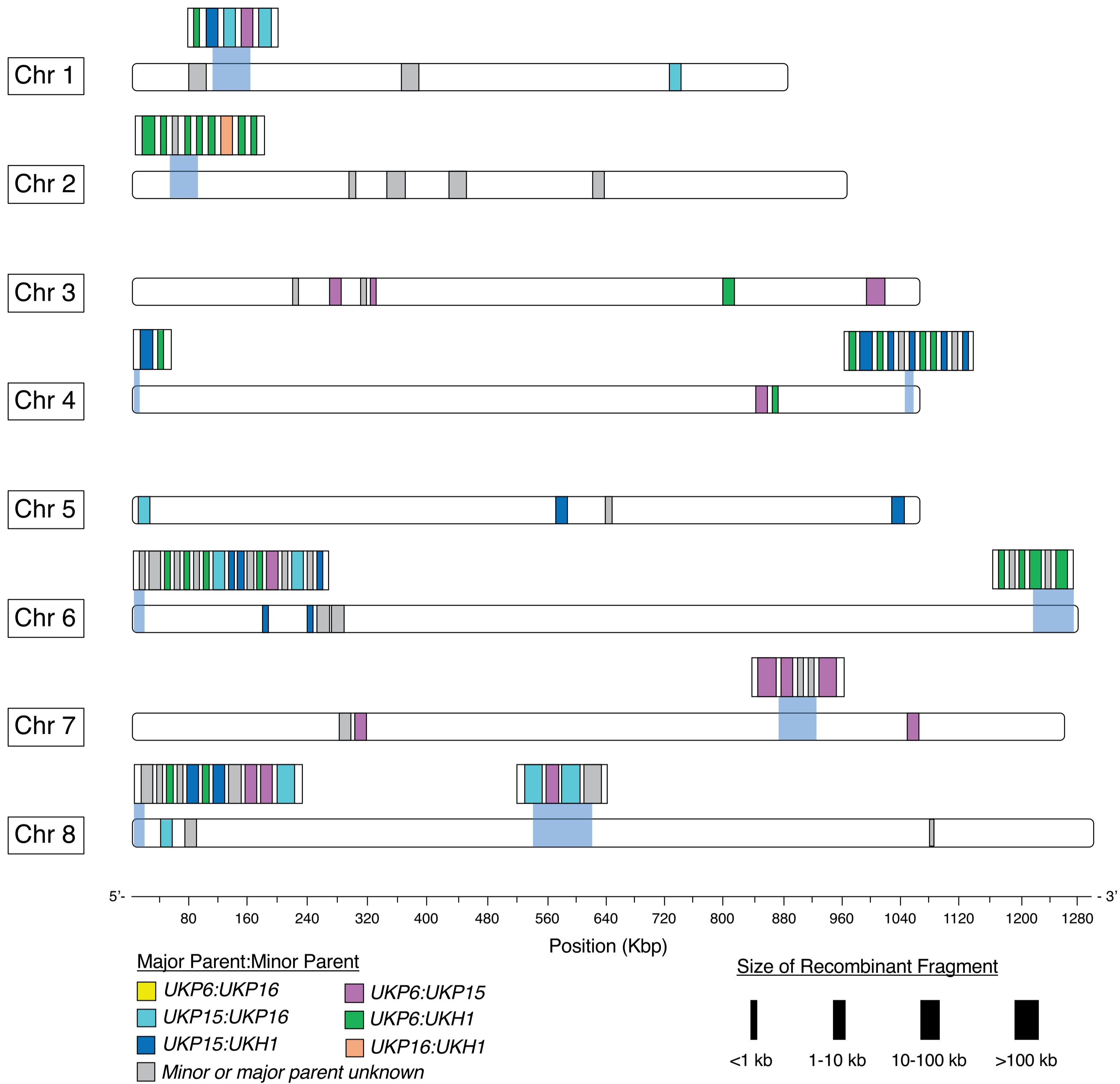
● *C. p. parvum* UKP6 v. *C. hominis* UKH4 ● *C. p. parvum* UKP6 v. *C. p. parvum* UKP16
● *C. p. parvum* UKP6 v. *C. p. anthroponosum* UKP15 ● *C. p. parvum* UKP6 v. *C. p. parvum* UKP8

b

● *C. p. parvum* UKP6 v. *C. hominis* UKH4 ● *C. p. parvum* UKP6 v. *C. p. parvum* UKP16
● *C. p. parvum* UKP6 v. *C. p. anthroponosum* UKP15 ● *C. p. parvum* UKP6 v. *C. p. parvum* UKP8

*ANOVA $p < 0.00001$ **c****d**

a**b****c****d****e**

a**b**